Acta Geologica Polonica, Vol. 70 (2020), No. 1, pp. 31–49
DOI: 10.24425/agp.2019.126457

The impact of a Neogene basaltoid intrusion on the distribution of rare earth elements and yttrium in Carboniferous rocks from the Sumina area, Poland (SW part of Upper Silesian Coal Basin)

ZDZISŁAW ADAMCZYK[1], JOANNA KOMOREK[1], JACEK NOWAK[1] and MAŁGORZATA LEWANDOWSKA[2]

[1] *Silesian University of Technology, Faculty of Mining, Safety Engineering and Industrial Automation, Department of Applied Geology Akademicka 2 Street, 44-100 Gliwice, Poland.*
[2] *Silesian University of Technology, Planning, Financial Analyses and Controlling Office, Akademicka 2 Street, 44-100 Gliwice, Poland.*
E-mails: zdzislaw.adamczyk@posl.pl; joanna.komorek@posl.pl; malgorzata.lewandowska@posl.pl; jacek.nowak@posl.pl

ABSTRACT:

Adamczyk, Z., Komorek, J., Nowak, J. and Lewandowska, L. 2020. The impact of a Neogene basaltoid intrusion on the distribution of rare earth elements and yttrium in Carboniferous rocks from the Sumina area, Poland (SW part of Upper Silesian Coal Basin). *Acta Geologica Polonica*, **70** (1), 31–49. Warszawa.

The Neogene basaltoid intrusions found in the S-7 borehole in the Sumina area (USCB) caused transformations of the adjacent Carboniferous rocks. The mineral and chemical compositions of the basaltoides are similar to those of the Lower Silesian basaltoides. The transformations that took place in the vicinity of the intrusion were manifested in the formation of natural coke, the secondary mineralization of these rocks (calcite, chlorite, zeolites and barite) and in the specific distribution of rare earths (REY). Among REY, the light elements (LREY) had the highest share, while the heavy elements (HREY) had the lowest share. Regardless of the lithological type of the analyzed rock, with increasing distance from the intrusion, the percentage of MREY and HREY elements increases at the expense of the light elements LREY. All analyzed distribution patterns of the REYs are characterized by the occurrence of anomalies, which often show a significant correlation with the distance of sampling points from the basaltoid intrusion. The specific distribution of REYs in the vicinity of the intrusion of igneous rocks is an indication of the impact of hydrothermal solutions associated with the presence of basaltoides on the rocks closest to them located at a temperature of over 200°C.

Key words: Rare earth elements and yttrium (REY); Neogene basaltoid intrusion; Upper Silesian Coal Basin (USCB).

INTRODUCTION

The peculiarities of contact metamorphism caused by an intrusion of magmatic melts may vary substantially, depending on the type of the intrusive body and the distance from it. In the Carboniferous deposits of the Upper Silesian Coal Basin (USCB), several occurrences of subvolcanic intrusion have been reported. The effects of the interaction of volcanic intrusions with country rocks, and with coal seams, have been described in many papers. The intrusions were mainly basaltic, and located in the southwest part of the USCB (Chodyniecka and Sankiewicz 1972, 1978; Duźniak *et al.* 1976; Jochemczyk 1984; Probierz *et al.* 1988;

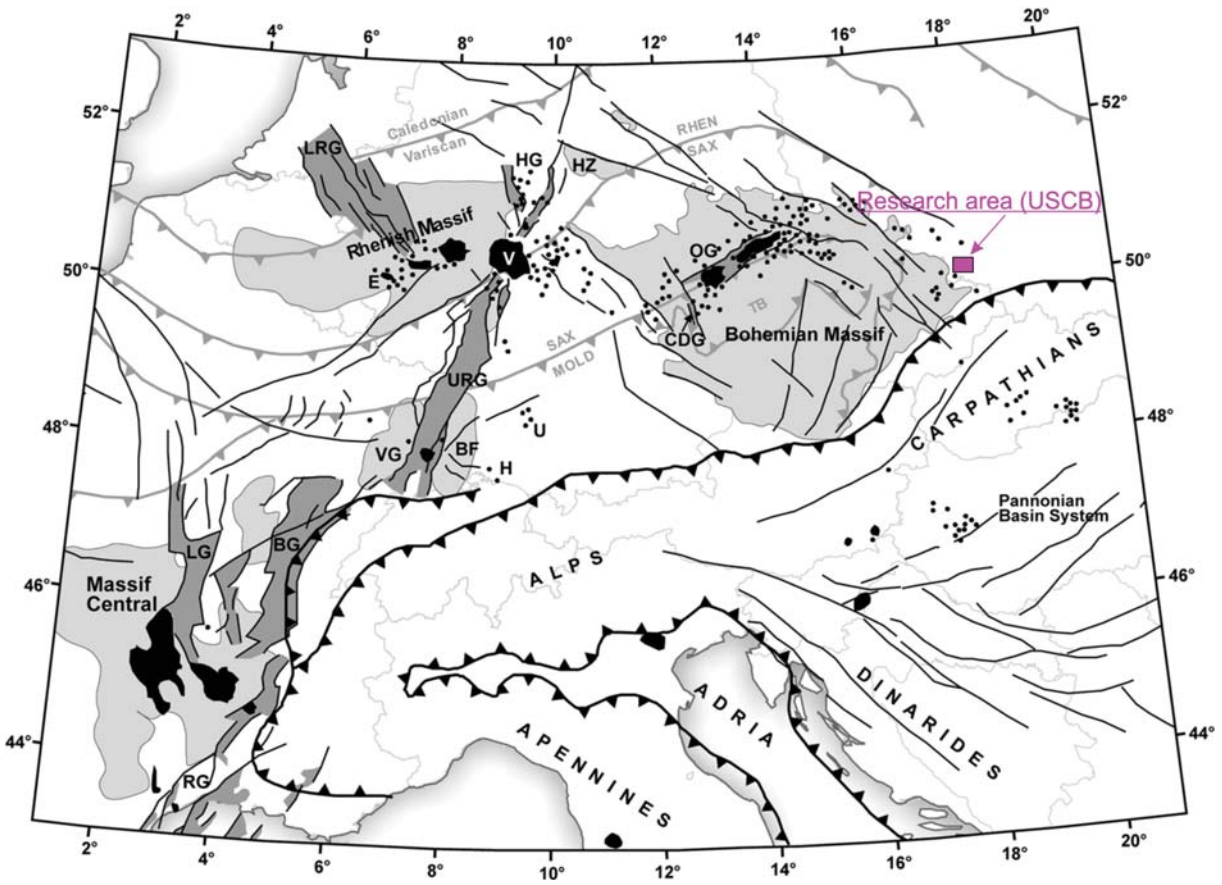

Text-fig. 1. The schematic map showing the distribution of Cenozoic volcanic areas (black fields and dots), main rift-related sedimentary basins (dark grey) and Variscan massifs (medium grey) in the Central European region. Important post-Variscan faults are shown as thin black lines, Alpine thrust front and main Variscan sutures are shown as black and grey barbed lines, respectively. Grabens and volcanic regions: BG – Bresse Graben, CDG – Cheb-Domažlice Graben, E – Eifel Mts., H – Hegau, HG – Hesse Graben, LG – Limagne Graben, LRG – Lower Rhine Graben, OG – OhřeRift Graben, RG – Lower Rhône Graben, U – Urach, URG – Upper Rhine Graben, V – Vogelsberg Mts. Variscanmassifs: BM – BohemianMassif, BF – Black Forest, HZ – Harz Mts., VG – Vosges Mts. Crustal segments of the Variscan orogen: RHEN – Rhenohercynian, SAX – Saxothuringian, MOLD – Moldanubian, TB – Teplá-Barrandian, USCB – Upper Silesian Coal Basin. Grabens, faults, and Alpine front in the western part of the map are taken from Dèzes *et al.* (2004) and Ulrych *et al.* (2011) with modifications

Probierz 1989; Kapuściński *et al.*1990; Gabzdyl *et al.* 1992; Kwiecińska 1992; Chodyniecka and Hanak 2000; Komorek *et al.* 2010; Matuszewska *et al.* 2015; Smędowski *et al.* 2015; Adamczyk *et al.* 2018).

An S-7 borehole drilled during exploratory works in the Sumina area, was located on the north-western slope of the Jejkowice Basin, and it passed through Quaternary sediments (clays and sands), Cenozoic rocks (sandy claystones with marl and gypsum interlayers) and Carboniferous formations represented by the marginal Gruszów Beds (Upper Mississippian). In the lithologically monotonous Carboniferous deposits, a complex of basaltoides was found, which had already been the subject of scientific research (Chodyniecka and Sankiewicz 1978; Adamczyk *et al.* 2018).

As previously demonstrated, the Gruszów Beds occur in the form of claystones with minor interbedding of mudstones and sandstones. Among this succession, at depths of 611.95–612.8, 626.9–627.70, and 710.70–711.60 m, basaltoid dykes were encountered. Their thicknesses were 0.85, 0.80 and 0.90 m, respectively (Text-fig. 1), and these intrusions were attributed with qualification to the Cainozoic Central European volcanic province.

The basaltoides have a holocrystalline porphyric texture and an unoriented microstructure, and the mineral compositions in the separate sections were very similar. The phenocrysts are made of idiomorphic pyroxene (augite) and olivine. It is also noteworthy that the phenocrysts were altered, something that

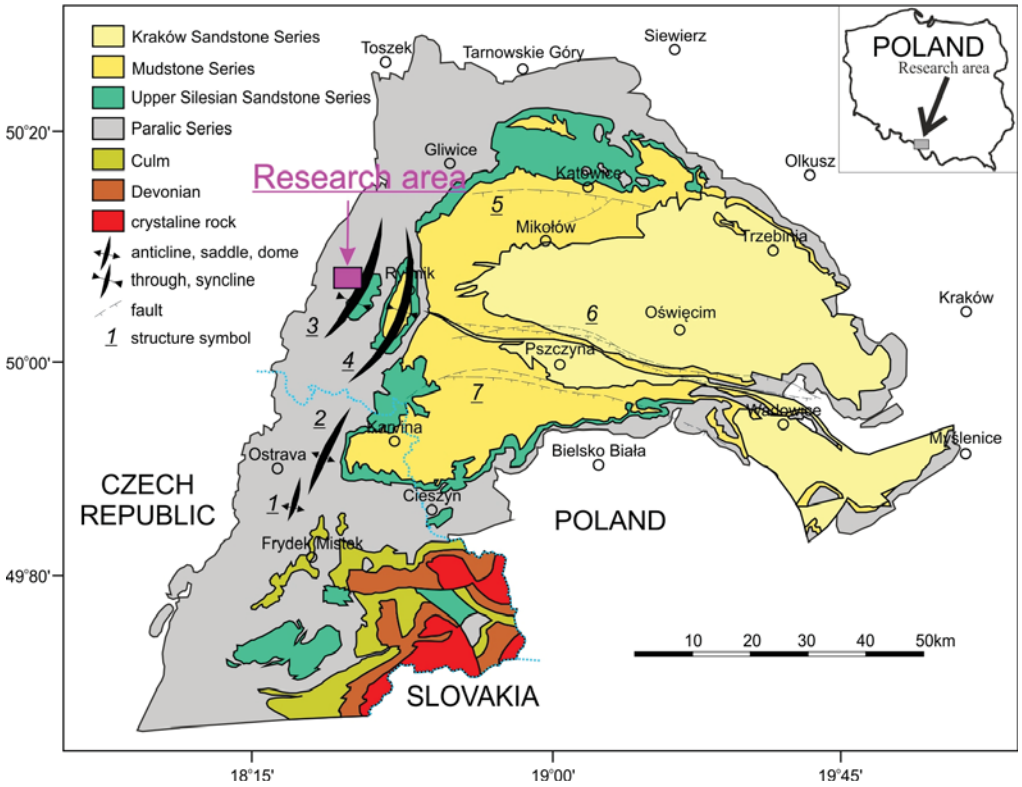

Text-fig. 2. The geological sketch of the Upper Silesian Coal Basin (Probierz *et al.* 2012, modified by Smędowski et. al. 2015), showing the location of the research area. Explanations: 1 – Michałkowice saddle, 2 – Orlova fold, 3 – Jejkowice trough, 4 – Chwałowice trough, 5 – Kłodnica fault, 6 – Żory-Piasek-Jawiszowice-Wysoka fault zone, 7 – Gorzyce-Bzie Zameckie-Czechowice-Kęty fault zone

is manifested by the presence of pseudomorphs of calcite, rarely of dolomite, chrysotile and antigorite after olivine. Sporadically, the phenocrysts of pyroxene were also altered and the products of this alteration were observed at their edges in the form of chlorites and iron oxides. Augite, magnetite, nepheline, and carbonates were found in the groundmass. These components are evenly distributed in the groundmass in form of fine crystals. Zeolites were also found in previously gas-filled pores.

Some former publications (Chodyniecka and Sankiewicz 1978; Adamczyk *et al.* 2018) indicated thatsandstone and claystone occurred in contact with intrusions. The only signs of contact metamorphism described in these publications were the formation of a glaze coat and natural coke occurring in coal-rich interlayers that accompanied the claystone, pointing to thermal metamorphism.

So far, in the publications describing the impact of the volcanic intrusions, thermal transformations of organic substances have usually been given more attention than the effects of metamorphism on the country rocks accompanying the coal seams and coal-rich interlayers. The most common result of thermal metamorphism of coal is its conversion into anthracite or natural coke.

In the case of the Sumina area, basaltoid intrusions display a direct contact with the country rocks that accompany the coal seams in the USCB; only in one case is there a contact with a thin coal interlayer. This enables the determination of the impact of basaltoid intrusion on country rocks, in particular on the distribution of rare earth elements in the zone of the impact of the basaltoid intrusion influence. Distribution of rare earth elements, in addition to thermal transformations of organic matter, may be a chemical indicator that determines the extent of this metamorphism in the surrounding rocks, as magma is the primary source of this group of elements.

This group includes 17 elements, i.e. 15 lanthanides (La, Ce, Pr, Nd, Pm, Sm, Eu, Gd, Tb, Dy, Ho, Er, Tm, Yb, and Lu) as well as Sc and Y. There are several classifications of these elements that take into account geochemical and economic considerations

(Seredin 2010; Seredin and Dai 2012). If yttrium is included, the following three subgroups are formed: light – (LREY: La, Ce, Pr, Nd, Pm, Sm), middle – (MREY: Eu, Gd, Tb, Dy and Y) and heavy – (HREY – Ho, Er, Tm, Yb and Lu). Yttrium in nature is closely associated with the lanthanides, since its ionic radius is similar to that of Ho and its ionic charge is equal to that of Ho. For this reason yttrium is sometimes placed in the REY distribution patterns between Dy and Ho (Bau 1996).

The REY distribution patterns are usually presented as graphs of REY concentration in the test samples normalized to standard materials, relative to their atomic number.

Due to their consistent behaviour in various geochemical processes, rare earth elements and yttrium have been widely used for many years as chemical indicators of the sedimentation environment and the history of coal deposits (Seredin 1996; Hower *et al.* 1999; Schatzel and Stewart 2003; Qi *et al.* 2007; Seredin and Finkelman 2008; Seredin and Dai 2012; Bau *et al.* 2014; Hower *et al.* 2015a, b; Dai *et al.* 2015, Dai *et al.* 2016).

The anomalies of the content of elements such as La, Ce, Eu, Gd and Y, and the enrichment or depletion of light – LREY, middle – MREY, or heavy – HREY elements are commonly used for the reconstruction of the geochemical history of the deposit (Hower *et al.* 1999; Mardon and Hower 2004).

The purpose of this work was to determine the distribution of rare earths and yttrium (REYs) within the contact zone of the basaltoid intrusion in the S-7 borehole in the Sumina area. Analysis of REY (L-, M-, H-type) enrichment types and of some anomalies will constitute an attempt to illustrate the geochemical impact of a basaltoid intrusion on rocks associated with coal seams in the Sumina area.

It should be noted that previously geochemical aspects were not examined in studies of the effects of contact metamorphism within the system of basaltoid intrusions and rocks accompanying coal seams in the USCB.

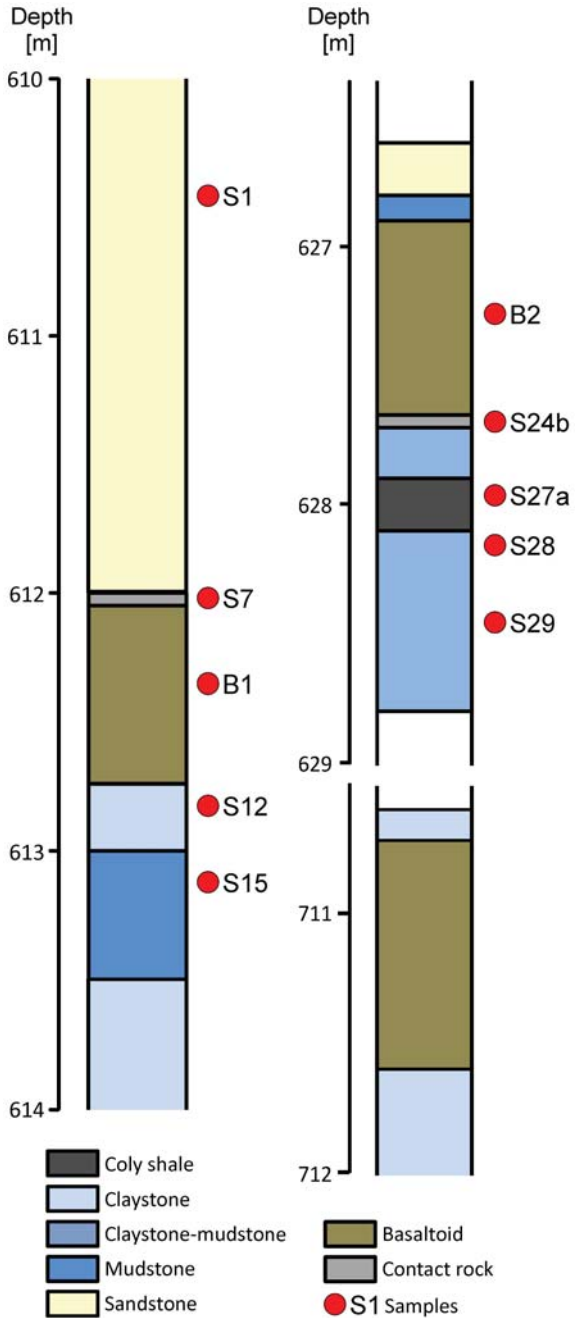

Text-fig. 3. Samples localization in the geological profile of the Sumina S-7 (USCB) with basaltoid intrusions

SAMPLING AND TESTING METHODS

Research was based on 10 core samples collected from a drill core of the S-7 borehole located in Sumina in the west part of the USCB (Text-fig. 2). The research included the determination of the mineral and chemical composition, including rare earth elements, of two basaltoid intrusions and the adjacent sedimentary rocks (country rocks) located both in their immediate vicinity and at some distance from the contact (Text-fig. 3).

Samples were represented by lithologies typical for the USCB rocks: sandstone (S1), claystones, and transition rocks of the claystone-mudstone, mudstone-sandstone type (S15, S28 and S29). Unusual for

the USCB Carboniferous deposits were basaltoids (B1 and B2) and the sedimentary rocks in contact with the basaltoid intrusions (S7, S12, S24b) or a sample in which the effect of this contact was observed (S27).

Mineral constituents were identified by means of microscope observations and X-ray diffraction method (XRD). A Zeiss transmitted light microscope with an image analyzer was used. A PANalytical AERIS 1 diffractometer with a $Cu_{K\alpha}$ lamp was used for XRD. Spectra were recorded within the 2θ angle range of 7° to 77° during the time of 4.84 seconds at 40 KV voltage and 8 mA current.

The content of the mineral components in the samples was determined using the Rietveld method and *HighScore Plus* computer software from Panalytical.

The chemical composition, including the content of rare earth elements, was determined using the ICP-MS method (inductively coupled plasma mass spectrometry) on a Perkin Elmer SCIEX ELAN 6000 ICP-MS spectrometer in Activation Laboratories Ltd. in Canada.

RESULTS AND DISCUSSION

Mineral composition

The sandstone in the analyzed profile (S1) is fine-grained and of light grey colour with black coal laminae and lenses. The mineral composition includes quartz, orthoclase, biotite, muscovite, plagioclase, rock clasts, and chlorite. The feldspars are present in the form of idiomorphic grains, with well preserved orthoclase, while plagioclases are partly illitized and carbonatized. Biotite flakes are partly sideritized and chloritized (Text-fig. 4A). The sandstone binder is argillo-siliceous with siderite admixtures. Clay minerals are represented by kaolinite (Text-fig. 5). The rock shows no signs of any transformation related to the presence of the basaltoid intrusion, although the presence of barite, ascertained by the XRD method, may represent the result of such alteration.

The thermally transformed claystone (S7), containing natural coke resulting from the impact of basaltoid intrusion B1, contains numerous vesicles and fissures filled with calcite, dolomite and zeolites (mainly philipsite), and chlorites (chamosite) (Text-fig. 4B), as well as barite detected by XRD (Text-fig. 5). This may be an indication of postmagmatic hydrothermal solutions that accompanied the basaltoid intrusions in the surrounding rocks (Adamczyk *et al.* 2018).

Basaltoid B1, as shown in the previous studies (Chodyniecka and Sankiewicz 1978; Adamczyk *et al.* 2018), is dark grey in colour and has a holocrystalline porphyric texture and an unoriented, slightly porous microstructure. Phenocrysts are represented by pyroxenes (Text-fig. 4C) and olivine, both of which usually were at various degrees of thermal transformation (chloritization, carbonatization, serpentinization). The groundmass contains pyroxenes (augite), magnetite, nepheline, and zeolites. Pores, of up to 50mm in size, contain crystallized carbonates (mainly calcite), zeolites, and chlorite.

In thermally transformed claystone S12, being dark grey in colour, and in contact with basaltoid B1, numerous pores filled with zeolites, calcite, and chlorite are present, as well as pseudomorphs of these minerals after pyroxenes and olivine. The claystone possibly contains laminae or lenses of organic matter. These have been transformed into natural coke, the process of which has been accompanied by the formation of devolatilisation pores, which were subsequently filled with secondary minerals (zeolite – philipsite, calcite, and chlorite, Text-fig. 5). Microscopic observations of the interface between basaltoid and claystone revealed the presence of a brown glazed coat (Text-fig. 4D).

The grey argillaceous mudstone S15 was seen to contain quartz, muscovite, biotite, organic matter (mainly in the form of laminae and lenses), and smaller quantities of orthoclase and rock clasts. The binder, in addition to silica, contains illite (Text-fig. 5). The rock shows no signs of transformations related to the basaltoid intrusion.

Basaltoid B2 was formed similarly to basaltoid B1. In addition, pyroxenes with optical properties of aegirine-augite (Text-fig. 4E), and fine grained amphiboles difficult to identify microscopically were found in the basaltoid. XRD helped identify olivines, and among the zeolites – philipsite and natrolite.

In the thermally transformed, graphite containing, grey coaly shale S24b, being in contact with basaltoid B2, and similarly to sample S12, numerous pores are filled with secondary minerals (calcite, zeolites and chlorite), as well as barite detected by XRD (Text-fig. 5). Coal is converted into natural coke. Sporadically, the natural coke contains pseudomorphs of secondary minerals after pyroxene phenocrysts (Text-fig. 4F).

Dark grey coaly shale S27a exhibited contact metamorphism in the form of natural coke occurrence. Numerous devolatilisation pores and fissures are filled, as was the case with samples S12 and S24b, with calcite and zeolites (Text-fig. 4G), rarely with chlorites. Barite is identified in this sample by XRD.

The grey argillaceous mudstone S28 resembles

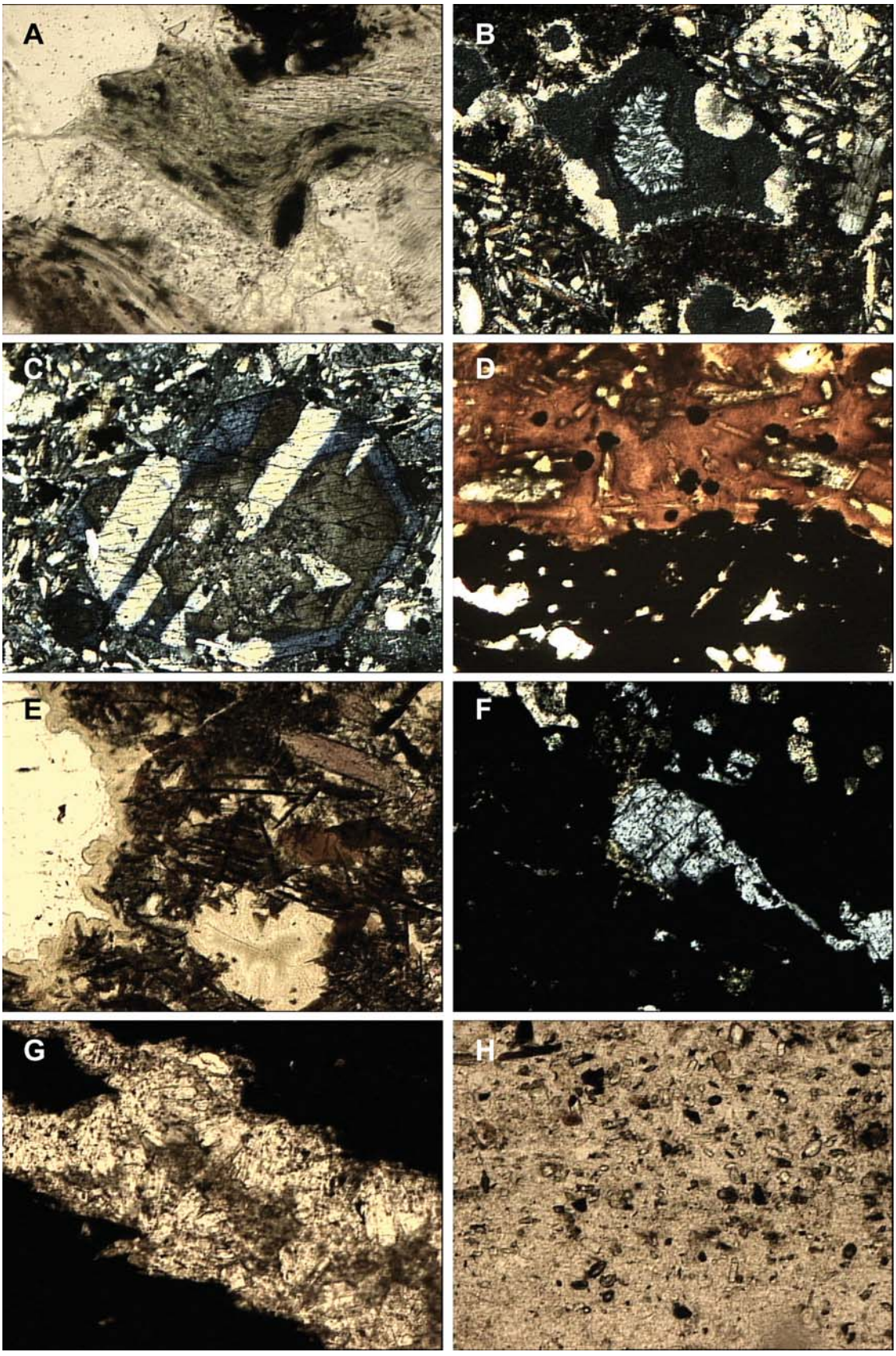
A
B
C
D
E
F
G
H

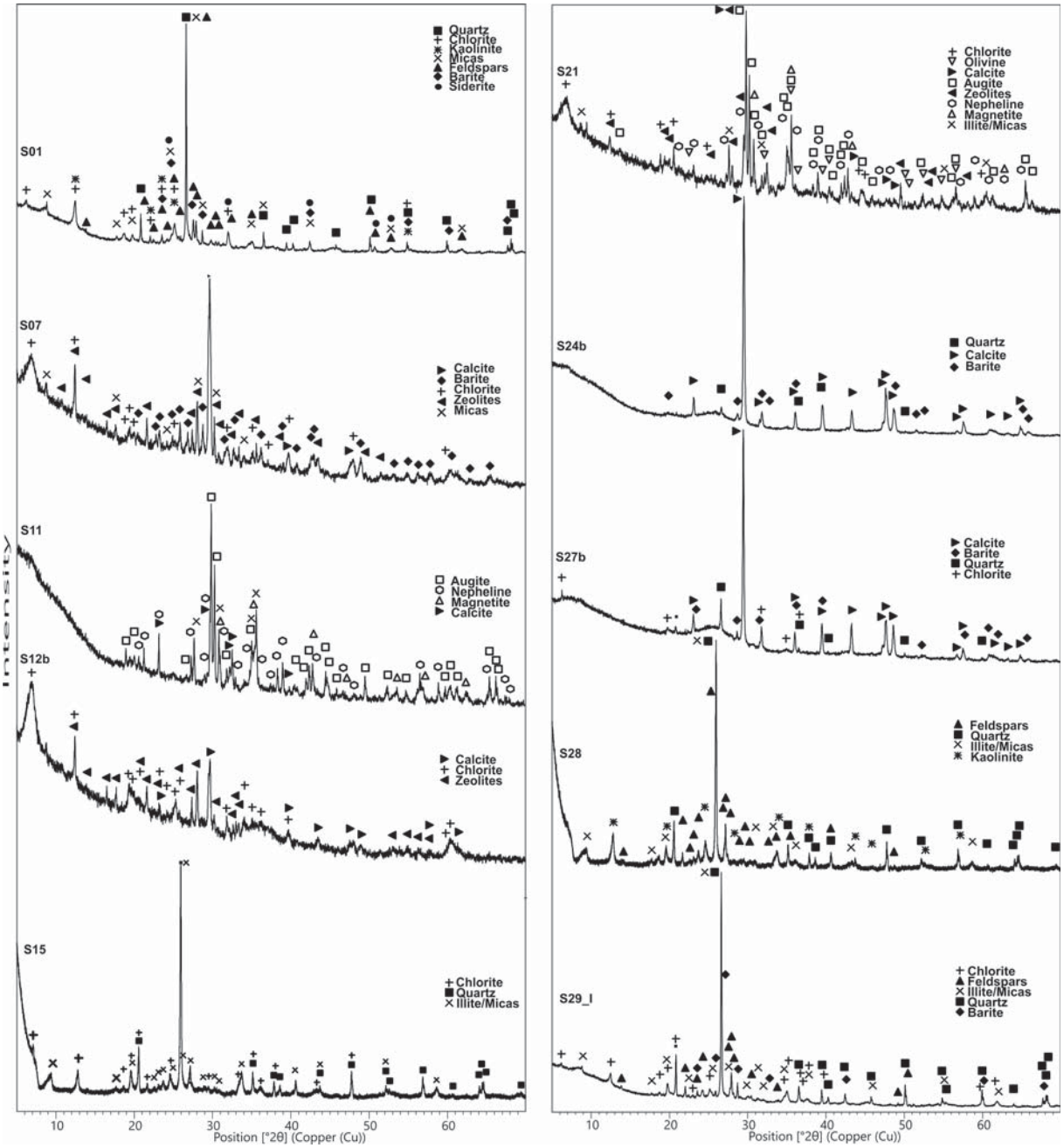

Text-fig. 5. X-ray diffractograms of analysed samples in the profile of the Sumina S-7

← Text-fig. 4. Microphotographs of rock samples in the profile of the Sumina S-7. A – Sample S1 – sandstone, biotite chloritization, PP light. B – Sample S7 – natural coke, pores filled with calcite, dolomite, zeolites and chlorite, XP light. C – Sample B1 – basaltoid, pyroxene phenocryst with concentric zoning and sector twins, XP light. D – Sample S12 – basaltoid-coke contact, coke covered with a brown glaze coat, PP light. E – Sample B2 – irregular zeolite-calcite-chlorite aggregates, violet pyroxene crystals (aegirine augite) and ilmenite dendrites on the right, PP light. F – Sample S24b – coke-basaltoid B2 contact, chlorite-zeolite pseudomorph after pyroxene, XP light. G – Sample S27a – a crack in coke filled with calcite and zeolites, PP light. H – Sample S29 – argillaceous mudstone with fine crystals of barite, PP light. Explanation: A-G magnification 100×, H magnification 200×; PP light – parallel polarisers, XP light – crossed polarisers

sample S15; it has an oriented microstructure emphasized by the presence of coal laminae. The following minerals are present in the rock: quartz, muscovite, and biotite, rock clasts, as well as orthoclase. Zircon and garnets clasts were found sporadically. The rock binder is siliceous argillic, with local siderite, chlorite admixtures. The clay mineral is kaolinite (Text-fig. 5).

Argillaceous mudstone S29 is grey in colour, and in terms of mineral composition it is similar to the sample S28; with some fine crystals of barite (Text-fig. 4H) and chlorite. Barite presence was detected in XRD spectra (Text-fig. 5).

Chemical composition

The major chemical constituents of the studied basaltoids are SiO_2, Al_2O_3, $Fe_2O_{3(tot.)}$, MgO, and CaO (Table 1). Their contents are within the ranges most commonly found in the Lower Silesian basaltoids (Text-fig. 6). The remaining main oxides (TiO_2, MnO, Na_2O, K_2O and P_2O_5) present in smaller quantities, although the high values of loss on ignition (LOI) are notable: 7.45 wt.% in sample the B1, and 8.14 wt.% in the sample B2. These high LOI values are mainly related to mineral composition of the basaltoids, principally to the presence of calcite, zeolites, and chlorite.

The chemical compositions of the country rocks in contact with basaltoids – samples S7, S12, and S24b – differ both from those of the basaltoid and of the other sedimentary rocks in the profile. This is due to the relatively high loss on ignition, which is related to the presence of large amounts of calcite, zeolites, chlorites, and organic matter identified by microscopic observations and XRD. High calcite content is also evidenced by the highest CaO shared among the examined Carboniferous samples. At the same time, the contact rock samples show relatively low Al_2O_3 and SiO_2 content as compared to that in both basaltoids and other rocks.

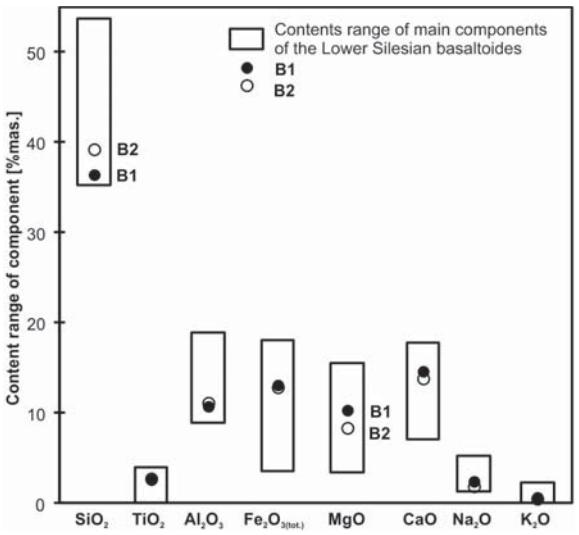

Text-fig. 6. Contents of main components in the basaltoides from Sumina region on the general background of the Lower Silesian basaltoides

Also noteworthy is the high proportion of BaO in the samples of the country rock-basaltoid boundary, being in the range of 0.42–2.92 wt.% (S7, S24b), apart from the sample S12 (0.04 wt.%). The BaO contents in the studied Carboniferous rocks from the Sumina area were compared with the average content in the Carboniferous rocks of USCB – the Załęże and Ruda s.s. Beds (Kokowska-Pawłowska 2018). It unequivocally indicates that sedimentary rocks from the

Chemical component	Sample									
	S1	S7	B1	S12	S15	B2	S24b	S27a	S28	S29
SiO_2	54.36	23.56	36.53	34.45	59.60	39.26	40.28	41.31	58.97	61.95
TiO_2	0.98	1.53	2.71	0.52	0.84	2.84	3.03	0.47	0.88	0.76
Al_2O_3	15.63	6.97	10.83	14.08	19.49	11.23	12.95	13.99	18.46	18.23
$Fe_2O_{3(tot.)}$	10.68	9.45	13.19	2.96	4.44	12.94	13.64	1.87	6.26	4.89
MnO	0.13	0.16	0.19	0.19	0.04	0.16	0.07	0.02	0.06	0.04
MgO	2.76	5.38	10.41	1.68	2.00	8.45	7.23	1.08	2.31	1.84
CaO	0.56	15.90	14.71	18.38	0.44	13.92	5.88	0.70	0.45	0.44
Na_2O	1.24	1.57	2.52	0.54	1.33	1.97	2.58	1.33	1.67	1.78
K_2O	4.22	0.80	0.75	3.18	4.27	0.60	0.62	2.62	3.41	3.30
P_2O_5	0.22	0.69	1.19	0.09	0.19	1.05	1.12	0.11	0.23	0.22
BaO	0.08	2.92	0.08	0.04	0.05	0.09	0.42	0.04	0.05	0.04
LOI	8.86	30.92	7.45	23.29	7.70	8.14	12.38	37.04	7.44	6.15
Total	99.71	99.85	100.57	99.41	100.39	100.64	100.20	100.58	100.19	99.65

Table 1. The chemical composition of examined samples (%mas.)

Sumina area usually have a higher BaO content than in the compared rocks, as the average for the latter, is in the range of 0.06 to 0.07 wt.%. It seems, therefore, that the presence of barite, which was documented in the mineral composition of the samples, is related to the effect of hydrothermal solutions derived from basaltoid intrusions.

The remaining rock samples (S1, S15, S28, and S29) displayed chemical compositions typical of their lithological counterparts from the USCB. Chemical constituents occur at similar concentrations, the dominating ones being SiO_2 and Al_2O_3. Only the high content of $Fe_2O_{3(tot.)}$ and high LOI in the sandstone sample S1 are noteworthy. This may be due to the presence of siderite.

Rare earth elements and yttrium (REY) in the rocks of the Sumina area

REY content in the analyzed rock samples varied between 157.68 (sample S1) and 380.94 ppm (sample B1) (Table 2). The highest REY content, over 300 ppm, was determined in basaltoid samples (B1, B2) and in the sample S24b from the basaltoid-country rock boundary. In other samples the REY concentration does not exceed 300 ppm. LREY concentration varies between 120.25 ppm (sample S1) and 327.70 ppm (sample B1). MREY content varies between 26.83 ppm (sample S7) and 56.26 ppm (sample S29). The samples have a heavy rare earth element (HREY) content, ranging from 4.23 ppm (sample S7) to 10.12 ppm (sample S29).

The studied Carboniferous rocks from the Sumina area usually show higher REY concentrations than those of the Carboniferous rocks of the USCB – the Załęże and Ruda s.s. Beds (Kokowska-Pawłowska 2018). And although, as in the case of sandstones, the average content of REY for the Załęże and Ruda s.s. Beds layers is 188 ppm, and for the sandstone sample S1 it is 157.68 ppm, in other cases the contents can be compared are as follows: argillaceous mudstone – 216 and 258 ppm (S15), 284 ppm (S28) and 296 ppm (S29); coal shale – 175 ppm and 321 ppm (S24) and 177 ppm (S27); claystones – 218 ppm and 207 ppm (S7) and 162 ppm (S12).

Among rare earth elements, the light elements (LREY) displayed the highest share (above 75%) in the total rare earth element budget. Heavy elements (HREY) have the lowest share, not more than 4% of the total REY budget (Text-fig. 7, Table 2).

Although the absolute content of rare earths and yttrium in the analyzed samples is differentiated, a significant negative correlation ($r = -0.77$, $p = 0.01$) was found between the percentage of LREY and the

Sample	Y	La	Ce	Pr	Nd	Sm	Eu	Gd	Tb	Dy	Ho	Er	Tm	Yb	Lu
	[ppm]														
S1	21	26.4	55.2	6.65	26.3	5.7	1.19	4.5	0.7	4.3	0.8	2.2	0.32	2.1	0.32
S7	15	44.3	82.2	8.86	34.0	6.3	1.53	5.6	0.7	4.0	0.7	1.7	0.23	1.4	0.20
B1	28	85.7	158.0	15.5	57.7	10.8	3.38	9.1	1.2	5.8	1.0	2.4	0.30	1.8	0.26
S12	20	32.2	59.0	6.25	24.3	4.9	1.01	4.1	0.6	3.8	0.8	2.1	0.31	2.0	0.31
S15	35	45.5	94.1	10.1	40.4	8.3	1.40	7.1	1.1	6.2	1.3	3.5	0.51	3.4	0.50
B2	29	74.2	142.0	14.2	54.8	10.1	3.31	9.1	1.2	6.0	0.9	2.5	0.31	1.8	0.27
S24b	19	77.0	136.0	13.0	47.3	8.8	2.45	7.1	1.0	5.0	0.8	2.0	0.25	1.4	0.18
S27a	21	33.3	67.3	7.17	27.7	5.6	0.97	4.4	0.6	3.5	0.7	2.0	0.31	2.0	0.29
S28	36	50.3	107.0	11.1	44.7	9.1	1.31	7.7	1.2	6.6	1.3	3.5	0.53	3.7	0.55
S29	38	52.2	110.0	11.7	46.3	9.5	1.36	8.4	1.3	7.2	1.4	3.8	0.55	3.8	0.57

Sample	REY	LREY	MREY	HREY	LREY	MREY	HREY	Eu_N/Eu_N^*	Gd_N/Gd_{N*}	Ce_N/Ce_N^*	La_N/La_N^*	La_N/Lu_N^*
	[ppm]				[%]							
S1	157.68	120.25	31.69	5.74	76.26	20.10	3.64	1.12	1.03	0.95	1.12	0.88
S7	206.72	175.66	26.83	4.23	84.97	12.98	2.05	1.34	1.23	0.94	1.31	2.36
B1	380.94	327.70	47.48	5.76	86.02	12.46	1.51	1.72	1.17	0.98	1.35	3.52
S12	161.68	126.65	29.51	5.52	78.33	18.25	3.41	1.10	1.09	0.94	1.39	1.11
S15	258.41	198.40	50.80	9.21	76.78	19.66	3.56	0.88	1.06	1.00	1.31	0.97
B2	349.69	295.30	48.61	5.78	84.45	13.90	1.65	1.77	1.20	0.99	1.39	2.93
S24b	321.28	282.10	34.55	4.63	87.81	10.75	1.44	1.52	1.10	0.97	1.38	4.56
S27a	176.84	141.07	30.47	5.30	79.77	17.23	3.00	0.96	1.11	0.99	1.23	1.22
S28	284.59	222.20	52.81	9.58	78.08	18.56	3.37	0.75	1.05	1.03	1.34	0.98
S29	296.08	229.70	56.26	10.12	77.58	19.00	3.42	0.74	1.07	1.01	1.26	0.98

Table 2. The REY content in the examined samples

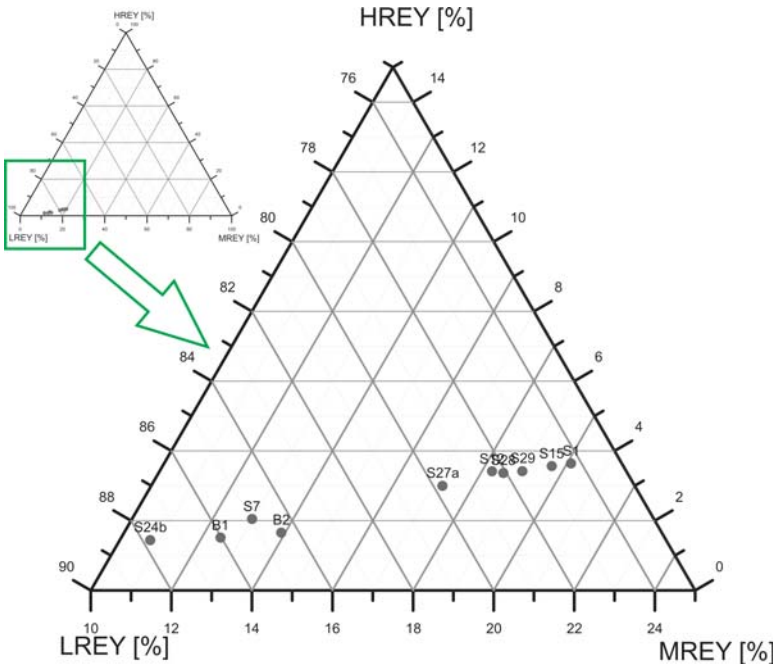

Text-fig. 7. The normalized concentrations of LREY, MREY and HREY in analyzed samples

distance of the sample from the basaltoid dyke (Text-fig. 8). Also significant strong correlations, although in these cases positive ones, are found between MREY r = 0.76, p = 0,01) and HREY (r = 0.80, p = 0.005) concentrations in the samples and the distance from the intrusion. This means that, regardless of the type of the analyzed sample, with increasing distance from the intrusion, the amount of MREY and HREY elements increases at the expense of LREY.

In order to determine the degree of enrichment of the samples in rare earths, the REY content determined in the samples is normalized against its content in reference rocks. The rocks most often selected for reference are those of a similar origin, which underwent similar geochemical differentiation during their formation. The content of rare earth elements is usually normalized against chondrites, and in the case of sedimentary rocks to the Upper Continental Crust – UCC (Taylor and McLennan 1985), North American Shale Composite – NASC (Gromet *et al.* 1984) or Post-Archaean Australian Shale – PAAS (Taylor and McLennan 1985).

Most of the analyzed rocks in the S-7 borehole profile in the Sumina area are sedimentary rocks, hence the normalization of REY content against UCC was applied here.

With regard to the distribution of REY in comparison to UCC, the samples may be classified into the following groups: enriched with: LREY – L type (ratio $La_N/Lu_N>1$), MREY – M type (ratio $La_N/Sm_N<1$ and $Gd_N/Lu_N>1$) and HREY – H type (ratio $La_N/Lu_N<1$). The distribution pattern of each type may have a positive or negative anomaly of different amplitudes for different elements because their behaviour in the environment may differ from that of other REYs. Subtypes and intermediate types can be distinguished with regard to occurring anomalies (Seredin and Dai 2012; Hower *et al.* 2013).

Analysis of the REY distribution in the samples has shown that the distribution patterns in basaltoids (samples B1 and B2) belong to the L-M type (Text-fig. 9). Similar characteristics (L-M type) also observed in samples taken at distances of 0.35 to 0.65 m from the basaltoid dykes (samples S7, S12, S24b and S27a). Distribution patterns determined for samples of other rocks taken at distances of 0.80 to 1.25 m from the intrusion have M-H type.

All analyzed REY distribution patterns are characterized by the various types of anomalies. In the case of distribution patterns in samples from the Sumina area, anomalies in Eu, Gd, La, and Ce were analyzed.

The obtained results show that some of the analyzed patterns are characterized by a bulge, mainly within the range between Nd and Y, with a maximum

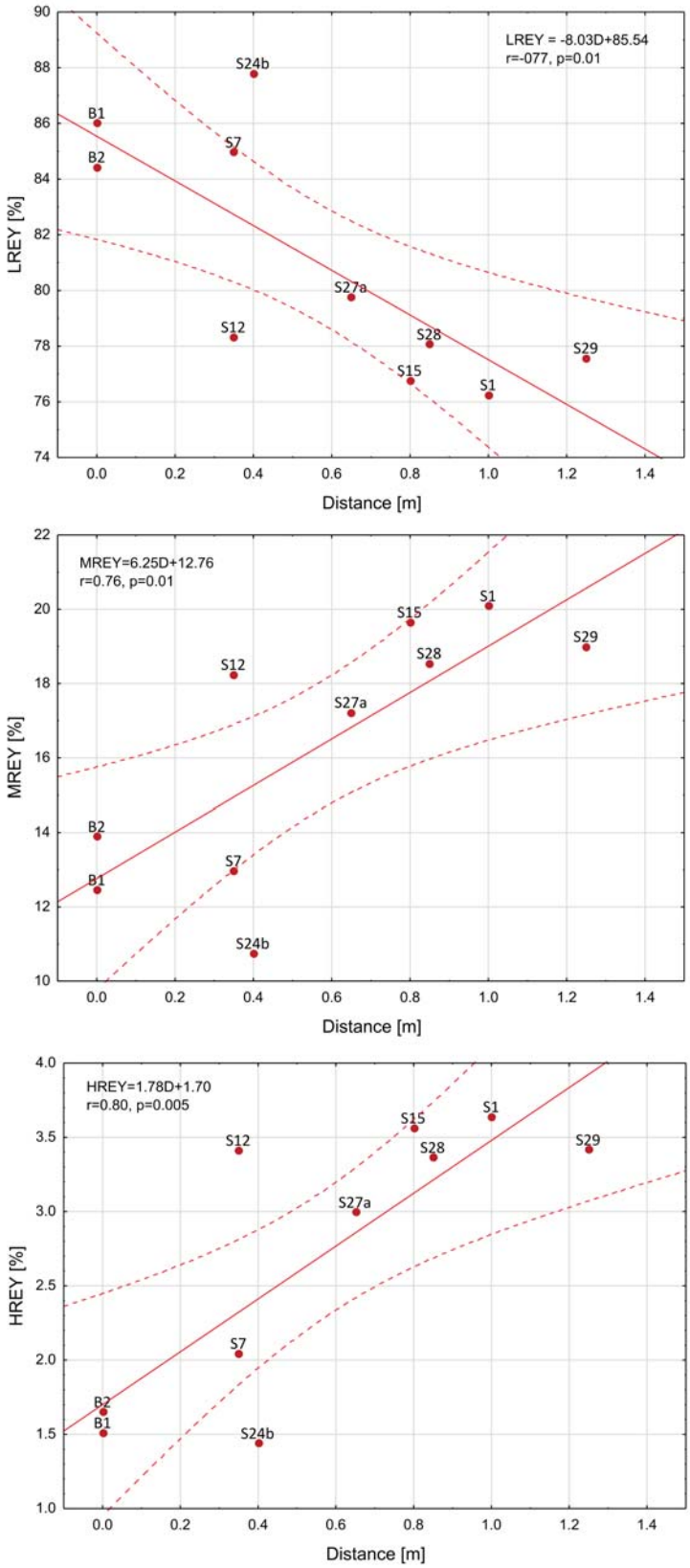

Text-fig. 8. The relationship between LREY, MREY i HREY content and the distance from the sampling point to the basaltoid dykes.

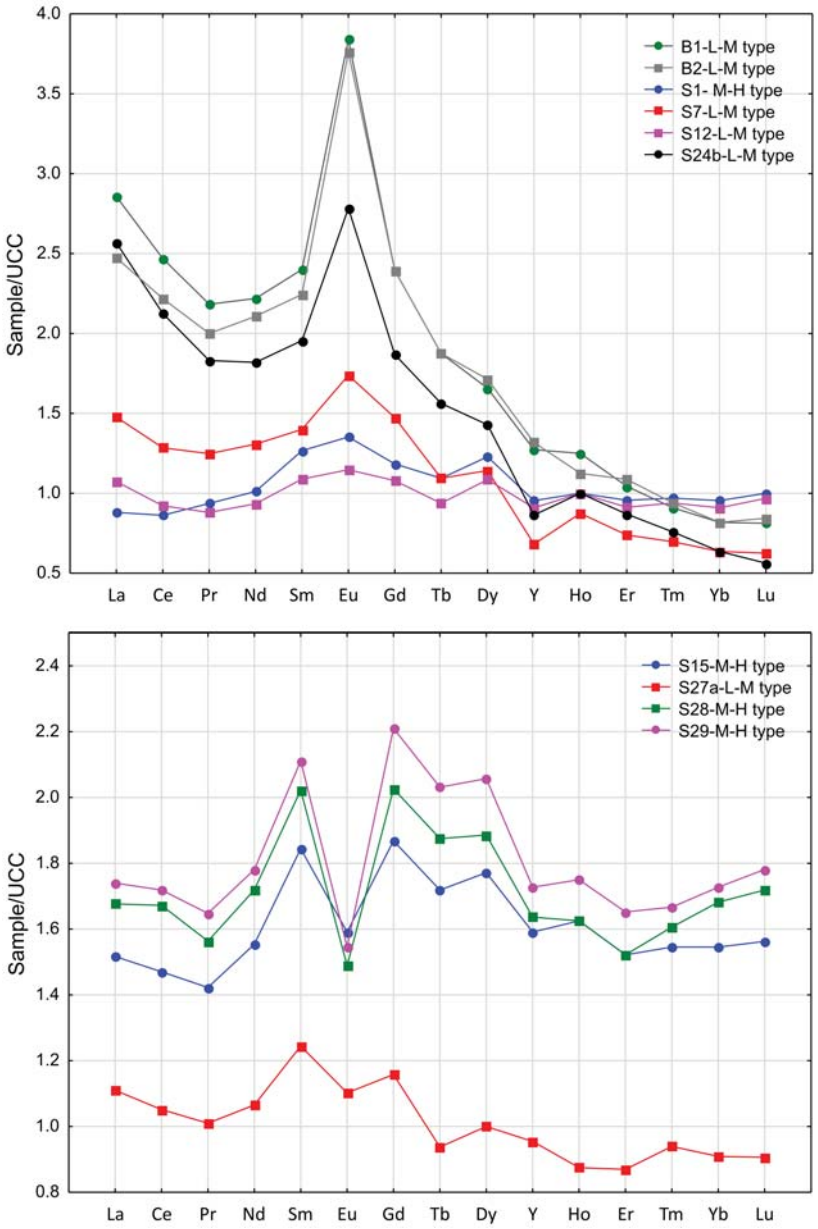

Text-fig. 9. Distribution patterns of REY in analysed samples. REY are normalized to average concentrations in Upper Continental Crust (UCC) (Taylor and McLennan 1985)

(positive anomaly) for Eu. These patterns were determined for samples B1, B2 S1, S7, S12, and S24b. Distribution patterns determined for samples S15, S27, S28, and S29 are characterized by a negative Eu anomaly.

The value of the europium anomaly for was determined from the formula (Dai *et al.* 2016):

$$Eu_N/Eu_N^* = Eu_N/(0.67 \cdot Sm_N + 0.33 \cdot Tb_N) \quad (1)$$

Application of the above formula helped to avoid interference of this anomaly with an anomaly for gadolinium.

The value of the positive Eu anomaly varies from 1.10 in sample S12 to 1.77 in sample B2 (Table 2). The highest Eu anomalies of 1.72 and 1.77 were determined in samples B1 and B2, respectively. Positive Eu anomalies of 1.10 and 1.52 were also found in rock samples S1, S7, S12 and S24b. The value of the Eu

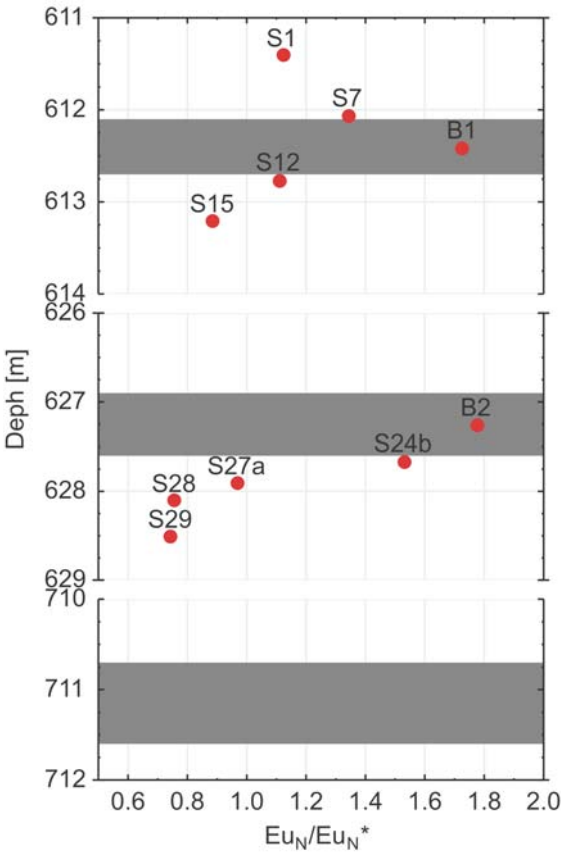

Text-fig. 10. Distribution of Eu anomaly value in in the profile of the Sumina S-7

negative anomaly varied from 0.74 in sample S29 to 0.96 in sample S27a.

A significant negative correlation (r = -0.88, p = 0.0008) was found between the value of Eu anomaly and the distance from the sampling point to the basaltoid dyke (Text-figs 10 and 11). The results obtained indicate that nearly all distribution patterns of samples taken at over 0.60 m from the basaltoid intrusion showed a negative Eu anomaly. The sample S1 taken 1 m away from the basaltoid dyke represents the single exception and has a positive Eu anomaly.

The positive Eu anomalies in sedimentary rocks may result from the action of hydrothermal solutions associated with the igneous rocks, e.g. igneous intrusions. Sedimentary rocks that have been subjected to the impact of basaltoid intrusions are characterized by positive Eu anomalies (Xiao *et al.* 2004; Bau *et al.* 2014; Dai *et al.* 2016).

The presence of a negative Eu anomaly may indicate that the rock was subjected to the action of hydrothermal solutions at a temperature of less than 200°C. On the other hand, a strong positive Eu anomaly would be expected when temperature of hydrothermal solutions was higher than 200°C acted on the rock (Dai *et al.* 2016). This relationship is confirmed by the distribution of Eu anomalies in the studied profile.

All analyzed distribution patterns are characterized by the occurrence of a positive Gd anomaly. This

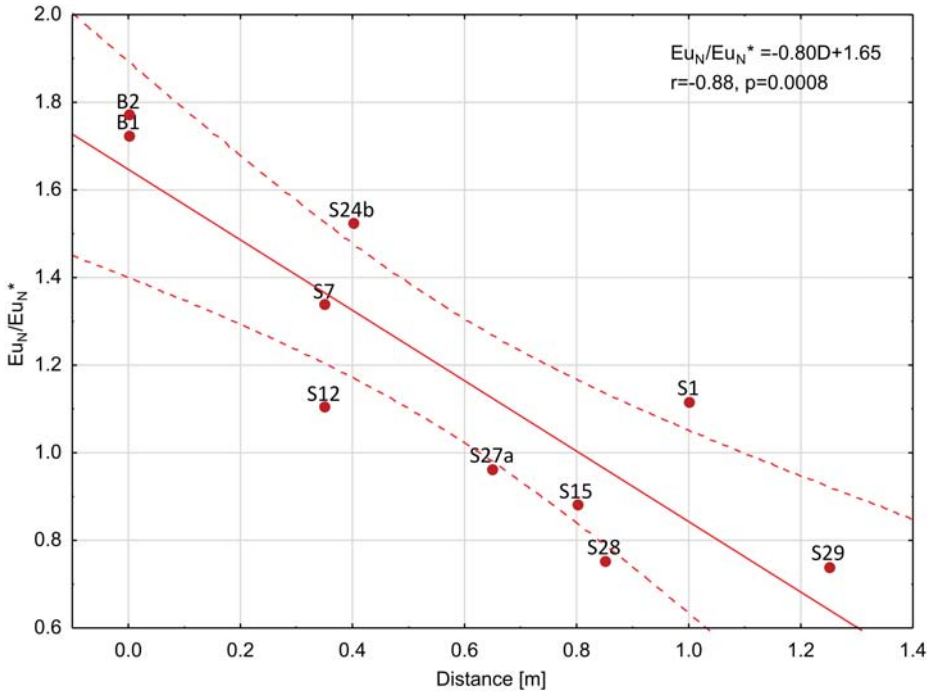

Text-fig. 11. The relationship between Eu anomaly value and the distance from the sampling point to the basaltoid dykes.

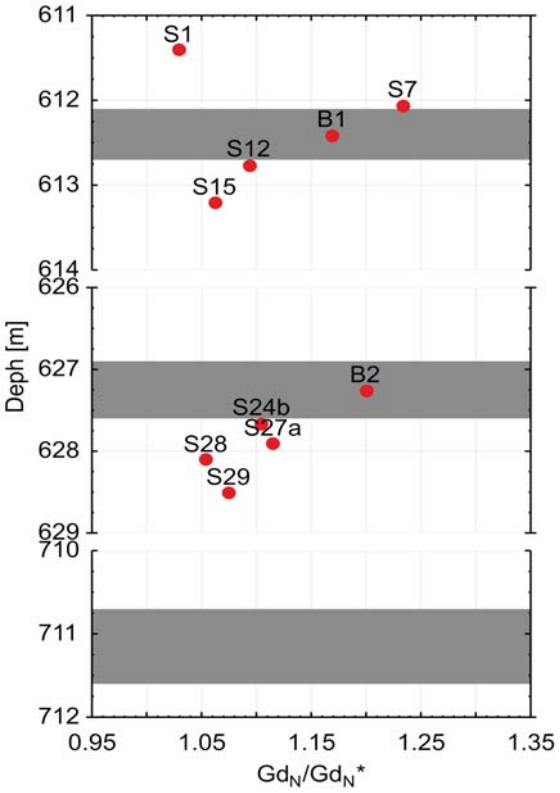

Text-fig. 12. Distribution of Gd anomaly value in in the profile of the Sumina S-7

anomaly is very pronounced in patterns in which a negative Eu anomaly was found. In patterns with a positive Eu anomaly, the Gd anomaly partially overlaps with the Eu anomaly (samples S15, S27a, S28 and S29).

The value of the Gd anomaly was determined from the formula (Bau and Dulski 1996; Dai *et al.* 2016):

$$Gd_N/GdN^* = Gd_N/(Sm_N \cdot 0.33 + 0.67 \cdot Tb_N) \quad (2)$$

The value of the positive Gd anomaly varied from 1.03 in sample S1 to 1.23 in sample S7 (Table 2). The basaltoid samples B1 and B2 have high values of this anomaly, 1.17 and 1.20, respectively. In other rock samples, the Gd anomalies have lower values between 1.03 (sample S1) and 1.11 (sample S27a).

A significant negative correlation (r = -0.77, p = 0.01) was found between the value of the Gd anomaly and the distance from the sampling point to the basaltoid dykes (Text-figs 12 and 13). Our results indicate that all samples taken at points over 0.70 m from the basaltoid intrusion have Gd anomaly values less than 1.10. The occurrence of this anomaly is most often related to the impact of sea water, of hydrothermal solutions, and of other waters on rocks (Bau 1996). All these factors cause the appearance

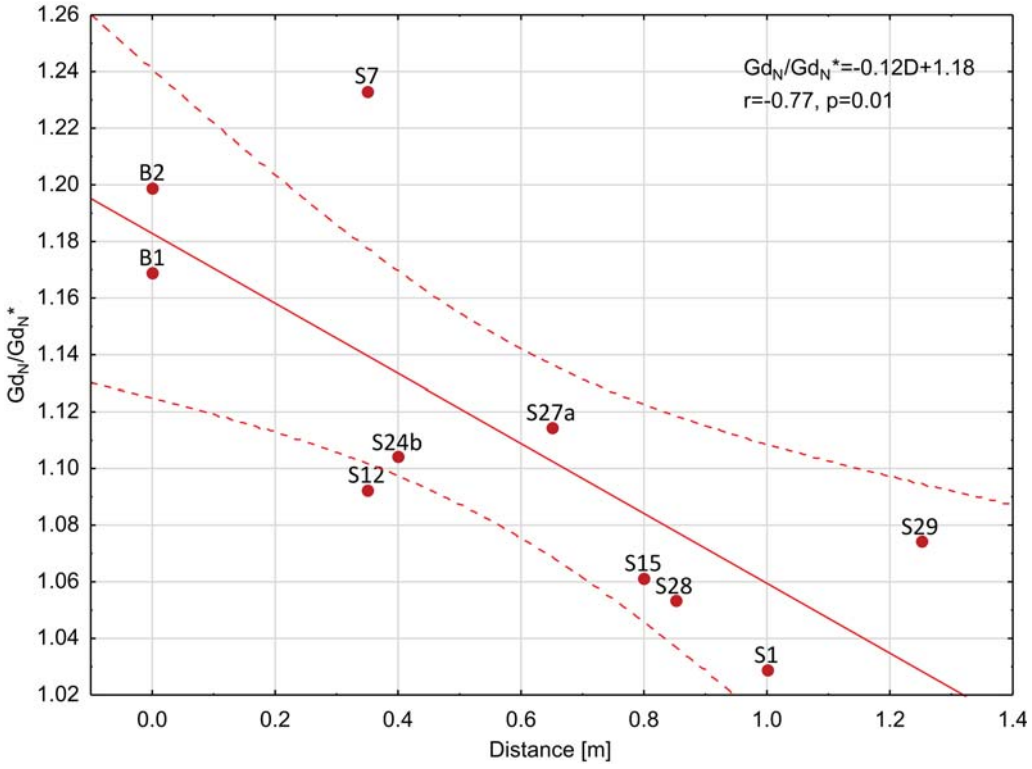

Text-fig. 13. The relationship between Gd anomaly value and the distance from the sampling point to the basaltoid dykes

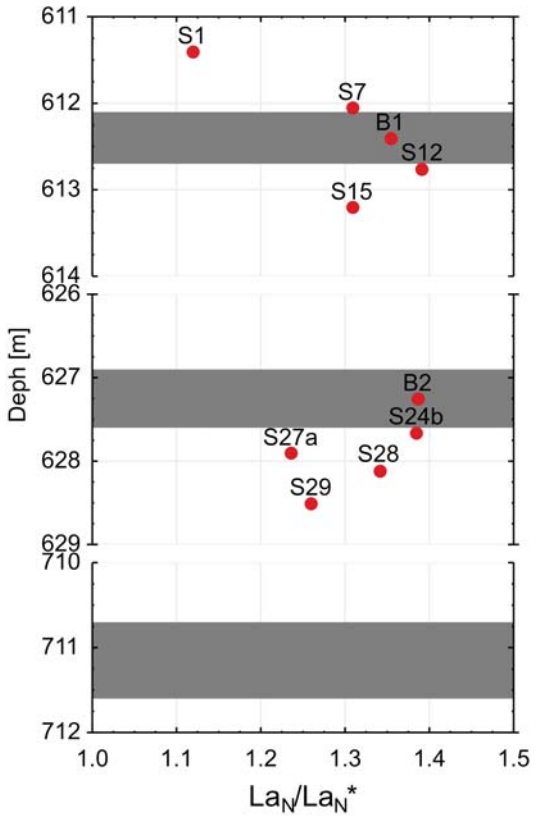

Text-fig. 14. Distribution of La anomaly value in in the profile of the Sumina S-7

of a positive Gd anomaly. In the case of the analyzed samples, this anomaly is probably related to the impact of hydrothermal solutions that accompany the basaltoid intrusion.

All analyzed distribution patterns have a positive La anomaly, the value of which is determined from the formula (Bau and Dulski 1996; Dai *et al.* 2016):

$$La_N/La_N^* = La_N/(3 \cdot Pr_N + 2 \cdot Nd_N) \quad (3)$$

The value of the positive La anomaly varies from 1.12 in sample S1 to 1.39 in samples S12 and B2 (Table 2). The basaltoid sample B1 shows an anomaly of 1.35. It should be noted that in most of the samples, the value of this anomaly exceeds 1.30. Samples S1, S27a and S29 were exceptions, for them these values were equal to 1.12, 1.23 and 1.26, respectively.

The values of La anomalies determined for basaltoids are typical for basaltoids characterized by low or high Ti content (Dai *et al.* 2016). The content of TiO_2 in our the basaltoids was 2.71 and 2.84%, respectively.

A significant negative correlation (r = -0.67, p = 0.03) was found between the value of the La anomaly and the distance from the sampling point to the basaltoid dyke (Text-figs 14 and 15). High values of

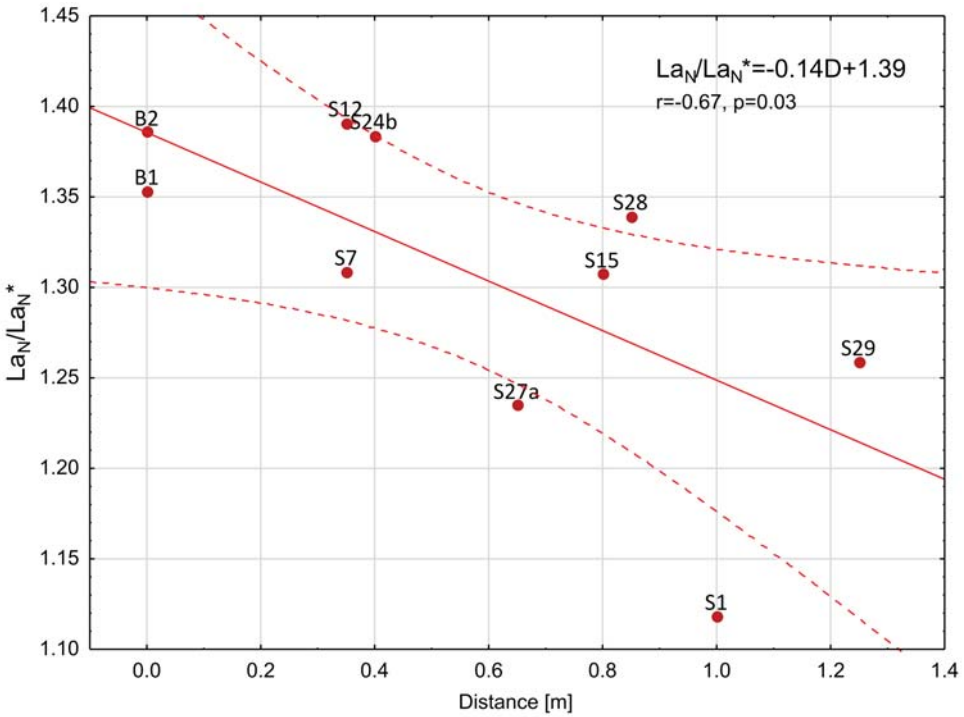

Text-fig. 15. The relationship between La anomaly value and the distance from the sampling point to the basaltoid dykes

the anomaly in rocks near the basaltoid dykes may indicate an effect of an interaction of igneous solutions with sedimentary rocks in the Sumina area.

All analyzed distribution patterns are characterized by Ce anomaly between 0.94 (sample S17 and S12) and 1.03 (sample S28) (Table 2). The value of this anomaly was determined from the formula (Bau and Dulski 1996; Dai *et al*. 2016):

$$Ce_N/Ce_N^* = Ce_N/(0.5 \cdot La_N + 0.5 \cdot Pr_N) \quad (4)$$

The results indicate that cerium in the analyzed samples shows either a weak positive, weak negative or no anomaly. In the case of this anomaly, no relationship was found, indicating no impact of basaltoid intrusion on the size of the anomaly (Text-fig. 16).

The ratio of normalized La_N/Lu_N content was analyzed in all samples. This ratio varied from 0.88 in sample S1 to 4.56 in sample S24b (Table 2).

In basaltoid samples B1 and B2 this ratio is equal to 3.52 and 2.93, respectively.

A significant negative correlation (r = -0.70, p = 0.02) exists between the La_N/Lu_N ratio and the distance from the sampling point to the basaltoid dykes (Text-figs 17 and 18).

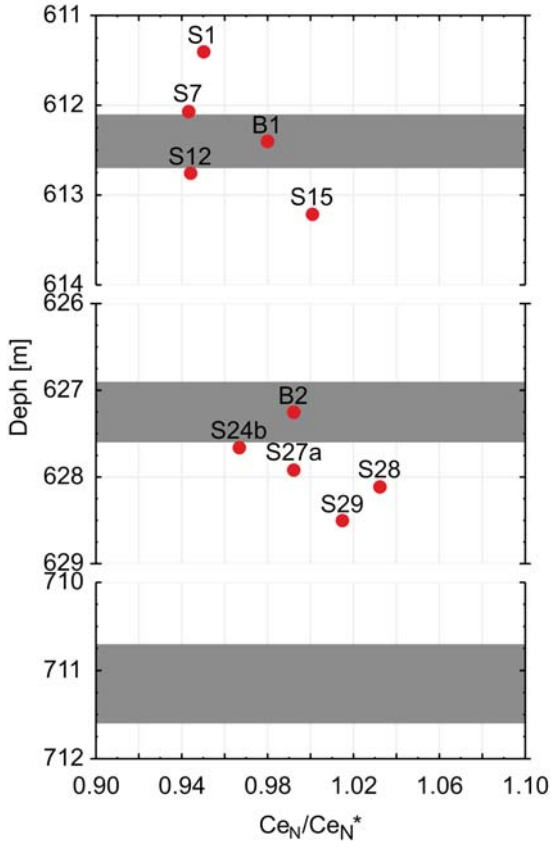

Text-fig. 16. Distribution of Ce anomaly value in in the profile of the Sumina S-7

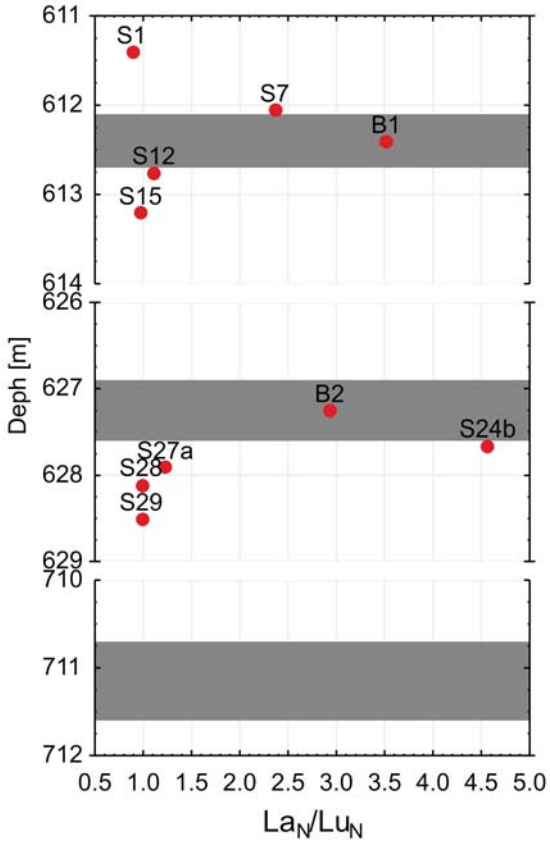

Text-fig. 17. The changes of the La_N/Lu_N ratio value in the profile of the Sumina S-7

The results obtained indicate that in samples taken at a point less than 0.70 m (S7, S12, S24b, S27a) from the basaltoid intrusion this value exceeds 1. These samples are also characterized by an REY distribution pattern of L-M type. In other samples this value is lower than 1 (between 0.88 and 0.98). These samples are also characterized by an REY distribution pattern of the M-H type.

CONCLUSIONS

The Neogene basaltoid intrusions intersected by the the S-7 borehole in the Sumina area (USCB) caused transformations of the adjacent Carboniferous rocks. The mineral and chemical compositions of the studied basaltoids are very similar to those of the Lower Silesian basaltoids.

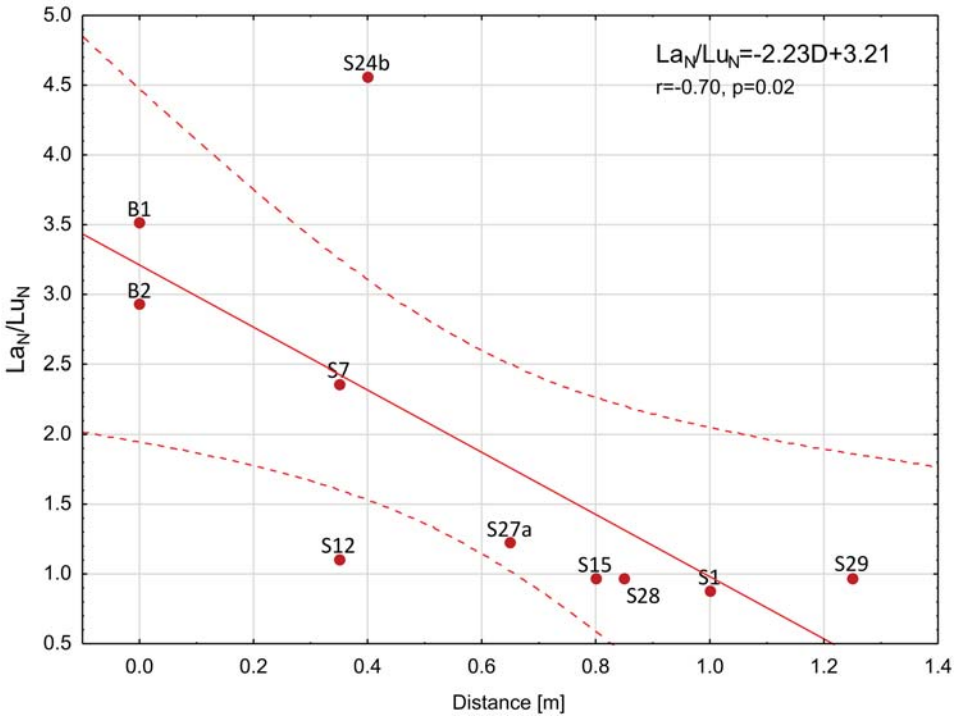

Text-fig. 18. The relationship between the value of La_N/Lu_N ratio and the distance from the sampling point to the basaltoid dykes

The transformations that took place in the vicinity of the intrusion were manifested in the formation of natural coke at the contact between country rocks and basaltoids, as well as in the secondary mineralization of these rocks, following the specific distribution of rare earths in vicinity of the intrusion.

Among the secondary minerals present in the Carboniferous rocks, calcite, chlorite and zeolites were found, as well as barite.

The studied Carboniferous rocks from the Sumina area usually show higher BaO and REY contents than those of the Carboniferous rocks of the USCB – the Załęże and Ruda s.s. Beds.

Among rare earth elements, the light elements (LREY) occupy the highest share (above 75% of all REYs), while the heavy elements (HREY) show the lowest share (< 4% of all REYs).

The results of the study indicate that regardless of the lithological type of the analyzed rock samples, with increasing distance from the intrusion, the percentage of MREY and HREY elements increases at the expense of the light elements LREY.

The distribution patterns determined for samples of basaltoids and country rocks taken at distances of up to 0.65 m from the basaltoid dykes display the characteristics of the L-M type. Distribution patterns determined for rocks located at distances of more than 0.80 m present the characteristics of the M-H type.

All analyzed distribution patterns of the REYs are characterized by the occurrence of various types of anomalies, which often show a significant correlation with the distance of sampling points from the basaltoid intrusions. This applies mainly to the anomalies of Eu, Gd, La, while the Ce anomaly does not show such a correlation.

The specific distribution of REYs in the vicinity of the intrusion of igneous rocks is an indication of the impact of hydrothermal solutions associated with the presence of basaltoids on the rocks closest to them. The temperature of these solutions is invoked to be higher than 200°C.

Acknowledgements

The authors would like to thank Professor Lidia Chodyniecka for providing rock samples from borehole Sumina S-7 for researches. The authors are grateful to reviewers for their valuable comments on the manuscript. Special thanks are to the journal editor Piotr Łuczyński for his editorial work.

REFERENCES

Adamczyk, Z., Kokowska-Pawłowska, M., Komorek, J., Klupa, A., Lewandowska, M. and Nowak, J. 2018. The impact of a Neogene basalt intrusion on the optical properties and internal structure of the dispersed organic matter in Carboniferous strata (SW-part USCB). *Acta Geologica Polonica*, **68**, 2, 249–262.

Bau, M. 1996. Controls of the fractionation of isovalent trace elements in magmatic and aqueous systems: evidence from Y/Ho, Zr/Hf, and lanthanide tetrad effect. *Contributions to Mineralogy and Petrology*, **123**, 323–333.

Bau, M. and Dulski, P. 1996. Distribution of yttriumand rare-earth elements in the Penge and Kuruman iron-formations, Transvaal Supergroup, South Africa. *Precambrian Research*, **79**, 37–55.

Bau, M., Schmidt, K., Koschinsky, A., Hein, J., Kuhn, T. and Usui, A. 2014. Discriminating between different genetic types of marine ferro-manganese crusts and nodules based on rare earth elements and yttrium. *Chemical Geology*, **381**, 1–9.

Chodyniecka, L. and Sankiewicz, J. 1972. Magmatic intrusion in Lower Namurian in the Marklowice region, Upper Silesia Coal Basin Poland (in Polish with English summary). *Rocznik Polskiego Towarzystwa Geologicznego*, **42**, 309–326.

Chodyniecka, L. and Sankiewicz, J. 1978. Basalts from the Suminy area (Rybnik coal basin) (in Polish with English summary). *Geological Quarterly*, **22**, 1, 119–128.

Chodyniecka, L. and Hanak, B. 2000. Intruzja z pokładu 414/3 w kopalni „Sośnica" (GZW) i jej wpływ na otaczający ją węgiel (in Polish). *Zeszyty Naukowe Politechniki Śląskiej, Górnictwo*, **246**, 55–71.

Dai, S., Seredin, V.V.,Ward, C.R., Hower, J.C., Xing, Y., Zhang, W., Song, W. and Wang, P. 2015. Enrichment of U-Se-Mo-Re-V in coals preserved within marine carbonate successions: geochemical and mineralogical data from the Late Permian Guiding Coalfield, Guizhou, China. *Mineral. Deposita*, **50**, 159–186.

Dai, S., Graham, I.T. and Ward, C.R. 2016. A review of anomalous rare earth elements and yttrium in coal. *International Journal of Coal Geology*, **159**, 82–95.

Dèzes, P., Schmid, S.M. and Ziegler, P.A. 2004. Evolution of the European Cenozoic Rift System: interaction of the Alpine and Pyrenean orogens with their foreland lithosphere. *Tectonophysics*, **389**, 1–33.

Duźniak, S., Gabzdyl, W. and Kapuściński, T. 1976. Intruzja bazaltowa i jej wpływ na węgiel w pokładzie 507 kopalni Sośnica (in Polish). *Przegląd Górniczy*, **12**, 524–528.

Gabzdyl, W., Pozzi, M. and Probierz K. 1992. Aspects of volcanism in the western part of Upper Silesian Coal Basin (Poland) and its influence on coal. *Acta Montana*, *seria: B Praha*, **2**, 86, 24–34.

Gromet, L.P., Dymek, R.F., Haskin, L.A. and Korotev, R.L. 1984. The "North American shale composite": its compilation, major and trace element characteristics. *Geochim. Cosmochim. Acta*, **48**, 2469–2482.

Hower, J.C., Ruppert, L.F. and Eble, C.F. 1999. Lanthanide, yttrium, and zirconium anomalies in the fire clay coal bed, Eastern Kentucky. *International Journal of Coal Geology*, **39**, 141–153.

Hower, J.C., Dai, S., Seredin, V.V., Zhao, L., Kostova, I.J., Silva, L.F.O., Mardon, S.M. and Gurdal, G. 2013. A Note on the Occurrence of Yttrium and Rare Earth Elements in Coal Combustion Products. *Coal Combustion and Gasification Products*, **5**, 39–47.

Hower, J.C., Groppo, J.G., Henke, K.R., Hood, M.M., Eble, C.F., Honaker, R.Q., Zhang, W. and Qian, D. 2015a. Notes on the potential for the concentration of rare earth elements and yttrium in coal combustion fly ash. *Minerals*, **5**, 356–366.

Hower, J.C., Eble, C.F., O'Keefe, J.M.K., Dai, S.,Wang, P., Xie, P., Liu, J.,Ward, C.R. and French, D. 2015b. Petrology, palynology, and geochemistry of Gray Hawk Coal (Early Pennsylvanian, Langsettian) in Eastern Kentucky, USA. *Minerals*, **5**, 592–622.

Jochemczyk, L. 1984. Skała ultramaficzna z warstw rudzkich rejonu Zebrzydowic (Rybnicki Okręg Węglowy). *Przegląd Geologiczny*, **8-9**, 443–445.

Kapuściński, T., Probierz, K., Kubik, A., Strzałkowska, E. and Drobiazgiewicz W. 1990. O występowaniu intruzji magmowej w warstwach siodłowych kopalni „Sośnica" (Górnośląskie Zagłębie Węglowe) i jej wpływie na węgiel pokładu 501/3. *Zeszyty Naukowe Politechniki Śląskiej, Górnictwo*, **187**, 97–115.

Komorek, J., Lewandowska, M. and Probierz, K. 2010. Peculiarites of petrographic composition of coking coals in southwest part of Upper Silesian Coal Basin (poland) as a results of thermal metamorphism influence. *Archive of Mining Sciences*, **55**, 4, 783–798

Kokowska-Pawłowska, M. 2018. Studium mineralogiczno-geochemiczne skał współwystępujących z węglem w pokładach 405 (warstwy załęskie) i 408 (warstwy rudzkie s.s.) w Górnośląskim Zagłębiu Węglowym, 719 p. Monograph. Wydawnictwo Politechniki Śląskiej; Gliwice.

Kwiecińska, B., Hamburg, G. and Vleeskens, J.M. 1992. Formation temperatures of natural coke in the Lower Silesian Coal Basin, Poland. Evidence from pyrite and clays by SEM-EDX. *International Journal of Coal Geology*, **21**, 217–235.

Mardon, S.M. and Hower, J.C. 2004. Impact of coal properties on coal combustion by-product quality: examples from a Kentucky power plant. *International Journal of Coal Geology*, **59**, 153–169.

Matuszewska, A., Pusz, S. and Duber, S. 2015. Evaluation of the structure of bituminous coal from Sośnica mine in the

Upper Silesian Coal Basin (Poland) using reflectance indicating surface (RIS) parameters *International Journal of Coal Geology*, **152**, 177–188.

Probierz, K., Pozzi, M., Kuci, P. and Płachecki K. 1988. Występowanie skał intruzywnych w stropie pokładu 403/4 KWK „Morcinek" (GZW). *Przegląd Górniczy*, **6**, 7–10.

Probierz, K. 1989. Wpływ metamorfizmu termalnego na stopień uwęglenia i skład petrograficzny pokładów węgla w obszarze Jastrzębia (GZW) (in Polish, detailed abstract in English). *Zeszyty Naukowe Politechniki Śląskiej, Górnictwo*, Gliwice, **176**, Monograph.

Probierz, K., Marcisz, M. and Sobolewski, A. 2012. Od torfu do węgli koksowych monokliny Zofiówki w obszarze Jastrzębia (południowo-zachodnia część Górnośląskiego Zagłębia Węglowego), 285 p. Wydawnictwo Instytutu Chemicznej Przeróbki Węgla; Zabrze.

Qi, H., Hu, R. and Zhang, Q. 2007. REE geochemistry of the Cretaceous lignite from Wulantuga Germanium Deposit, Inner Mongolia, Northeastern China. *International Journal of Coal Geology*, **71**, 329–344.

Schatzel, S.J. and Stewart, B.W. 2003. Rare earth element sources and modification in the Lower Kittanning coal bed, Pennsylvania: implications for the origin of coal mineral matter and rare earth element exposure in underground mines. *International Journal of Coal Geology*, **54**, 223–251.

Seredin, V.V. 1996. REE-bearing coals from Russian Far East deposits. *International Journal of Coal Geology*, **30**, 101–129.

Seredin, V.V. 2010. A new method for primary evaluation of the outlook for rare earth element ores. *Geology of Ore Deposits*, **52**, 428–433.

Seredin, V. and Finkelman, R.B. 2008. Metalliferous coals: a review of the main genetic and geochemical types. *International Journal of Coal Geology*, **76**, 253–289.

Seredin, V.V. and Dai, S. 2012. Coal deposits as potential alternative sources for lanthanides and yttrium. *International Journal of Coal Geology*, **94**, 67–93.

Smędowski, Ł., Duber, S. and Matuszewska, A. 2015. An effect of igneous intrusion on the structure, texture and microtexture of coal from the Sośnica coal mine, Upper Silesian Coal Basin, Poland. *Geological Quarterly*, **59**, 3, 507–516.

Taylor, S.R. and McLennan, S.H. 1985. The Continental Crust: Its Composition and Evolution, 312 p. Blackwell; Oxford.

Ulrych, J., Dostal, J., Adamovic, J., Jelinek, E., Spacek, P., Hegner, E. and Kadosa, B. 2011. Recurrent Cenozoic volcanic activity in the Bohemian Massif (Czech Republic). *Lithos*, **123**, 133–144.

Xiao, L., Xu, Y., Mei, H., Zheng, Y., He, B. and Pirajno, F. 2004. Distinct mantle sources of low-Ti and high-Ti basalts from the western Emeishan large igneous province, SW China: implications for plume-lithosphere interaction. *Earth and Planetary Science Letters*, **228**, 525–546.

Manuscript submitted: 9th July 2019
Revised version accepted: 25th September 2019